



# Neutronics and Photonics Study of Fusion Reactor Blankets

M.A. Abdou and C.W. Maynard

April 1974

UWFDM-97

Presented at the 1st Topical Meeting on the Technology of Controlled Nuclear Fusion,  
San Diego CA, 14-18 April 1974.

***FUSION TECHNOLOGY INSTITUTE***

***UNIVERSITY OF WISCONSIN***

***MADISON WISCONSIN***

# **Neutronics and Photonics Study of Fusion Reactor Blankets**

M.A. Abdou and C.W. Maynard

Fusion Technology Institute  
University of Wisconsin  
1500 Engineering Drive  
Madison, WI 53706

<http://fti.neep.wisc.edu>

April 1974

UWFDM-97

Presented at the 1st Topical Meeting on the Technology of Controlled Nuclear Fusion, San Diego CA,  
14-18 April 1974.

# Neutronics and Photonics Study of Fusion Reactor Blankets

M. A. Abdou  
and  
C. W. Maynard

Nuclear Engineering Department  
University of Wisconsin  
Madison, Wisconsin 53706

FDM 97

Paper presented at the First Topical Meeting on the Technology  
of Controlled Nuclear Fusion held in San Diego - April 14-18, 1974.

## Neutronics and Photonics Study of Fusion Reactor Blankets

M. A. Abdou\* and C. W. Maynard\*

The University of Wisconsin, Nuclear Engineering Department, Madison  
Wisconsin 53706

### I. Introduction

The choice of materials and the detailed design of CTR blankets is a complex process involving a number of technical areas such as neutronics, radiation damage, heat transfer, induced activity and afterheat, and economics. The neutronics analysis is of prime importance as it provides the basic input for almost all of the other studies.

A CTR blanket can usually be divided into three parts: 1- first wall and structure, 2- tritium breeding and energy conversion zone (which must have lithium in one form or another), and 3- a reflector region. The neutronics parameters of interest are nuclear heating, energy multiplication, gas production, atomic displacements, as well as tritium breeding.

In section II, a comparative study of several structural materials proposed for use in CTR blankets is carried out. Section III considers the question of increasing the energy production in the blanket. A comparison of the nuclear performance of several materials in the reflector region is presented in section IV. The nuclear design of the shield region is investigated in another paper<sup>1</sup> in these proceedings.

### II. First Wall and Structure

Several non-magnetic materials have been proposed for use as first wall and structural materials in the blanket. The strongest candidates are vanadium, niobium, molybdenum, stainless steel (SS), and SAP. The first three are refractory metals and it is very likely that alloys such as Nb-1Zr, V-20 Ti, or TZM alloys will be used rather than the pure metals. The neutronics and photonics results presented in this work are not affected significantly by low concentrations of alloying materials.<sup>2</sup> SAP (Sintered Aluminum Product) is 90% pure aluminum strengthened by about 10% by weight  $Al_2O_3$  and its utilization in fusion systems has been proposed<sup>3</sup> as a competitor to vanadium<sup>4</sup> from the points of view of low long term radioactivity and afterheat.

To compare the nuclear performance of these materials, a series of neutronics and photonics calculations were carried out for the blanket configuration shown in figure 1, with the first wall and structural materials as V, Nb, SS, SAP, and Mo. The calculations were run for the configuration shown in figure 1, with lithium of natural abundance and an additional shield region consisting of 70% Pb + 30%  $B_4C$ . All the neutron and gamma transport calculations were carried out in one-dimensional cylindrical geometry with ANISN<sup>5</sup> using the  $S_6$ - $P_3$  approximations.<sup>2</sup> The neutron and gamma multigroup cross sections were processed from ENDF/B3<sup>6</sup> with SUPERTOG<sup>7</sup> and MUG<sup>8</sup>, respectively. The neutron kerma factors and partial cross sections were processed with MACK<sup>9</sup> from ENDF/B3 except in the case of Mo where they were derived from Pearlstein's calculated cross sections.<sup>10</sup> Gamma production cross sections were processed with LAPHANO.<sup>11</sup>

### Tritium Production

The first part of table I compares the tritium breeding ratio,  $T$ , in Nb, V, SS, SAP, and Mo systems. From these results, it follows that the tritium breeding ratio is highest in vanadium with a  $T$  of 1.46 and lowest in niobium with a  $T$  of 1.27, and intermediate in SS, SAP, Mo systems. For a doubling time of about 7 years and allowing for losses in access regions (divertor, fueling passages, etc.) and uncertainties in nuclear data, a  $T$  of about 1.15 to 1.2 seems prudent as a design basis in one-dimensional calculations. Thus, it seems very unlikely that any uncertainty in nuclear data or in required amounts of structural materials will cause D-T fusion reactors to fail to produce sufficient fuel for their own needs and for initial fueling of other fusion reactors in an expanding power industry.

Assuming tritium production is potentially greater than the minimum for feasibility, the extra neutrons can be diverted to other purposes. The purposes and the materials used to achieve these goals become important. For example, one can attempt to produce excess tritium for fueling special fusion reactors which consume but do not produce tritium (these might be desirable for safety or environmental reasons). In addition, at least one alternative is to produce exothermic nuclear reactions and thus maximize the energy production per fusion reaction. This spreads the resource usage over more materials, lowers plant cost per unit power, and helps alleviate the materials problems of the first wall by reducing the neutron wall loading for a given plant power. Maximizing the blanket energy multiplication is dealt with in sections III and IV.

### Nuclear Heating

In table I, comparable data is presented for the neutron, gamma, and total nuclear heating by zone and for the entire blanket in units of MeV per D-T neutron for Nb, V, SS, and SAP systems. Accurate calculation of the nuclear heating in molybdenum from the present ENDF/B version III evaluations is not possible at present for two reasons: 1- absence of data on charged particle producing reactions (these contribute about 50% or more to neutron heating<sup>12</sup>), and 2- gamma production cross sections are not provided, and hence it is not feasible to calculate the gamma heating.

From the results in table I, the heating rate in niobium is about 2.3 times that in vanadium, twice the value in SAP, and 1.2 times that in a stainless steel first wall. This suggests that adequate cooling of the first wall may be simpler in vanadium and SAP than in niobium. However, this advantage is partially offset by the fact that niobium (also TZM can be operated at considerably higher temperatures (900° - 1000°C) than vanadium and much higher than SAP (350° - 400°C).

For a neutron wall loading of  $1 \text{ MW/m}^2$ , the average power density in the first wall is about  $12 \text{ watts/cm}^3$ , of which roughly 92% comes from absorption of secondary gammas. The gamma energy deposition in niobium is highest because it has the largest atomic number and secondary gamma source among the materials under consideration. It is of interest to note that the relative magnitude of the gamma and total heating in the first wall increases in these materials with the atomic number. The ratio of the neutron to gamma heating varies from roughly 10% in niobium to 215% in SAP.

Comparison of the total energy deposition in the blanket shows that using niobium increases the energy production by about 1 MeV over stainless steel and 0.6 MeV over SAP systems. This is a nontrivial gain since an increase of 1 MeV in the energy production per fusion reaction represents about 5% increase in the reactor power output. The origin of the better energy production with niobium compared to the other materials under consideration is the reaction  $Q$ -values for those reactions in which conversion of kinetic energy into mass or vice versa occurs. In a  $\text{Nb}(n,2n)$  reaction only 8 MeV is converted to mass while in the other materials more than 11 MeV is lost as nuclear mass. The  $(n,p)$  reaction is exothermic in niobium, but is endothermic in V, SS, and SAP. The  $\text{Nb}(n,\alpha)$  reaction results in a gain of 4.9 MeV while a loss of 2 to 3 MeV occurs through this reaction in vanadium and SAP and a gain of only about 0.3 MeV occurs in SS.

From the above results, it follows that the total recoverable energy (nuclear heating plus the 3.5 MeV kinetic energy of the alpha particle) per D-T neutron is, about 19 to 20 MeV in CTR blankets employing natural lithium. This is about an order of magnitude lower than the energy release per fission reaction. Hence, for the same thermal power, fusion reactors are required to produce far more neutrons than fission reactors. From an economics point of view, it is essential then in the design of CTR blankets to maximize the energy production per fusion reaction. Possible ways of accomplishing this goal is discussed in detail in later sections.

#### Gas Production and Atomic Displacements

First wall and structural materials are subjected to a high energy neutron flux which is much greater than that in any existing nuclear system. Therefore, radiation damage to the first wall of a CTR may be the most difficult technological problem once plasma confinement is assured. Assessment of radiation damage in fusion reactors requires information about the rates of gas production, transmutation, and atomic displacement.

For each zone, table II compares the reaction rates per D-T neutron for  $(n, \alpha)$ ,  $(n, n' \alpha)$ ,  $(n, p)$ ,  $(n, n' p)$ ,  $(n, d)$  and  $(n, t)$  reactions for the structural materials under consideration in the system of figure 1. A comparison of the gas production rates in appm/year ( $\text{MW}/\text{m}^2$ ) and atomic displacements per atom (dpa)/year ( $\text{MW}/\text{m}^2$ ) in Nb, V, SS, SAP, and Mo first walls is given in table III. The term ( $\text{MW}/\text{m}^2$ ) refers to the neutron wall loading. The helium production rate is the sum of  $(n, \alpha)$  and  $(n, n' \alpha)$  reaction rates. The rate of production of hydrogen isotopes is obtained by summing the results for the  $(n, p)$ ,  $(n, n' p)$ ,  $(n, d)$ , and  $(n, t)$  reactions. All cross sections were taken from ENDF/B3 <sup>6</sup> evaluations except those for Mo isotopes where cross sections theoretically calculated with Pearlstein's model<sup>10</sup> were used. In addition to Mo where all data on charged particle producing reactions is absent, no data is provided in ENDF/B3 for the  $(n, n' \alpha)$ ,  $(n, n' p)$ ,  $(n, d)$  and  $(n, t)$  reactions in Nb, V, and Fe or for the  $(n, n' \alpha)$  and  $(n, d)$  reactions in Ni and Cr. These reactions are marked by the letter N in table II and were taken as zero in obtaining the sum of the helium and hydrogen isotopes given in table III except for the case of Mo where the calculated cross sections were used. All the relevant data for aluminum and oxygen are provided in ENDF/B3.

The absence of nuclear data for some charged particle producing reactions must be carefully taken into consideration in comparing helium and hydrogen production rates for the structural materials. The results in table II show that the  $(n, n' p)$ , and  $(n, d)$  reactions contribute about 58 and 9%, respectively, to the production rate for hydrogen isotopes in a SAP first wall. The contribution of  $(n, n' \alpha)$  reaction to helium production is also significant. The results for molybdenum show that the  $(n, d)$  and  $(n, t)$  production rates are 16% and 4%, respectively, of the total hydrogen production rate. Thus it is almost certain that the gas production rates given in table III for Nb, V, and SS are underestimated.

Table III shows that helium and hydrogen production rates vary considerably from one material to another and is highest in SAP and lowest in niobium first walls. The helium production rates in Nb, Mo, V, SS, and SAP vary in the following proportion 1:2:2.4:8.6:17.7. Similar ratios for hydrogen are 1:1.2:1.3:6.7:9.8. Figures 2 and 3 show the spatially dependent hydrogen and helium production rates, respectively, in the five materials. These figures show that the relative magnitude of gas production in these materials does not vary appreciably with depth in the blanket except in the case of molybdenum. Figures 2 and 3 also show that the gas production rates decrease by more than an order of magnitude in the 42 cm (95% Li + 5% structure) blanket. It can also be noted from figures 2 and 3 that the gas production drops more rapidly in the first wall than in the lithium-structure region reflecting the fact that all five materials moderate neutrons more efficiently than lithium. This indicates that radiation damage will vary considerably in structural components in the blanket. Undesirable effects may arise such as differential swelling which will result in large stresses. The variation of damage implies also that the

frequency of replacing the structural components in the outer regions of the blanket may be less than that for the first wall.

The number of displacements per atom (dpa) per year for a  $1 \text{ MW/m}^2$  neutron wall loading is compared in table III for these same materials. The displacement cross sections used are given in reference 14, and were derived using mean displacement energies,  $E_d$ , of 60, 62, 40, 40, and 26 eV for Nb, Mo, V, SS, and Al respectively. These displacement energies are not accurately known, but the dpa rates in table III can be renormalized as they are inversely proportional to  $E_d$ .

The results show that the displacements per atom per year per ( $\text{MW/m}^2$ ) is about 14, 12, 10, 8, and 7 in SAP, V, SS, Mo, and Nb first walls, respectively. Thus the dpa rate variation from one material to another is less than the corresponding variation in gas production. The spatially dependent displacement rate in the five materials is shown in figure 4. This figure shows that the dpa rates in all materials drop within the blanket by about an order of magnitude indicating again the variation of damage to the structural components in the blanket.

Except for comparative purposes, the absolute values of gas production and displacement rate have little value unless translated into radiation damage terms. This is carried out in another paper.<sup>14</sup>

### III. Lithium Region and Energy Multiplication

As indicated earlier, increasing the energy production per fusion neutron is very desirable from an economics point of view. As shown in the last section, tritium production is potentially greater than the value required for a reasonable doubling time and a fraction of the neutrons can be diverted for the purpose of increasing energy multiplication. Maximizing the energy production in the blanket per D-T neutron results in reduced cost per unit power by either increasing power output at fixed wall loading and approximately fixed capital costs; or by reducing the wall loading while maintaining the power output. The latter results in lower radiation damage rates in the first wall and reduces the frequency of wall replacement. The associated improvement in plant availability (in addition to better reliability and safety) results in reduced unit power costs.

Fission-fusion symbiosis has been proposed<sup>15</sup> for the purpose of increasing energy multiplication, but the more complicated safety and maintenance aspects of such systems is a strong disadvantage. Although the subject of maximizing energy production in fusion systems deserves exhaustive studies, in the following only two concepts for achieving this by maximization of exothermic reaction rates are discussed.

Since lithium has to be employed in one form or another it is logical to try to maximize the exothermic reactions in lithium. Natural lithium consists of 7.42%  $^6\text{Li}$  and 92.58%  $^7\text{Li}$ . The dominant reaction in  $^7\text{Li}$  is the  $(n, n'\alpha)$  reaction which is important as high energy with a Q-value of -2.467 MeV. The most important reaction in  $^6\text{Li}$  is the  $(n, \alpha)$  which has a large  $1/v$  cross section at low energy and is exothermic with a Q-value of 4.785 MeV. The effect of enriching lithium (increasing the isotopic ratio of  $^6\text{Li}$ ) on energy multiplication in the blanket is brought out by a series of neutronics calculations for the system shown in figure 1 with a vanadium first wall and structure. The isotopic ratio of  $^6\text{Li}$  in lithium was increased from the natural abundance of 7.42% (design 401) to 15% in design 402, 30% in design 403 and 50% in design 404. The total energy produced in the system (first wall, lithium blanket, and reflector region) is given as a function of Li enrichment in table IV. The results show that the gain in energy multiplication as the  $^6\text{Li}$  isotopic ratio is increased is only 0.06% for 15%  $^6\text{Li}$ , and 0.5% for 50%  $^6\text{Li}$ . Given the fact that isotopic enrichment is an expensive process, these results imply that the economics for lithium enriched systems of configurations similar to that of figure 1 may differ little from systems operating with natural lithium. The reason the increase in energy

multiplication is small can be explained by analyzing the rates of exothermic and endothermic reactions. Due to the absence of a large  $(n,2n)$  reaction rate in the blanket, the increase in the  ${}^6\text{Li}$   $(n,\alpha)$  reaction rate is modest. Further, the gain in this reaction is partially offset by the increase in the rate of the  ${}^6\text{Li}$   $(n,n')$  endothermic reaction. Since  ${}^6\text{Li}$  is less efficient in moderating high energy neutrons than  ${}^7\text{Li}$ , increasing the  ${}^6\text{Li}$  isotopic ratio in lithium enhances the high energy endothermic reactions in the vanadium structure and stainless steel reflector. Table IV also shows the effect on the tritium breeding ratio of enriching the lithium. The results show that it does not change significantly and is optimal at about a 15% isotopic ratio of  ${}^6\text{Li}$ .

Since the  ${}^6\text{Li}$   $(n,\alpha)$  reaction rate per D-T neutron can not be increased beyond unity in the absence of  $(n,2n)$  reactions, the increase in energy production in lithium above 14 MeV is limited to 2 or 3 MeV because of unavoidable losses due to endothermic reactions in structural materials and  ${}^7\text{Li}$ . The next possibility for increased energy multiplication is to increase the number of neutrons by adding a material with a large  $(n,2n)$  reaction cross section. In order for the gain in energy to be significant the threshold for this reaction must be much less than twice the Q-value for the  ${}^6\text{Li}$   $(n,\alpha)$ , i.e. much less than 9.6 MeV and the material should not have other comparable endothermic reactions. The only material that satisfies these requirements is beryllium.

Design 401 described earlier with a first wall and structure of vanadium was chosen for investigating the effects of adding beryllium to the blanket. The basic design was kept the same, but an amount of Be equivalent to a 4 cm thick layer was homogenized with the first lithium region which is 20 cm of 95% natural lithium plus 5% vanadium. The new design was given the identification number 405. Design 406 is the same as 405 except that the equivalent beryllium thickness was increased to 10 cm. Table IV compares the results for neutron, gamma, and total heating as well as the effect on the tritium breeding ratio. It can be seen that the tritium breeding ratio in natural lithium increases from 1.46 in design 401 (no Be) to 1.68 in design 405 (4 cm Be) to 1.91 in design 406 (10 cm Be). The increases in the total energy production per D-T neutron is significant and is 9.3% and 18.45% when 4 cm and 10 cm of Be, respectively, are added.

Since adding 4 cm of Be increases the plant power output by about 10%, the cost of Be (about 60\$/lb at present) is no problem. However, the known resources of Be are limited to  $2 \times 10^4$  metric tonnes in the U.S.<sup>16</sup> A 4 cm thick layer of Be in a toroidal reactor with minor and major radii of 5 and 15 meters consumes about 1% of these resources. On the other hand, indications<sup>16</sup> are that world prospective resources may be 0.6 megatons. If this proves to be true, then a few hundred fusion reactors can utilize beryllium without exhausting a large fraction of the reserves.

The effects of enriching lithium in the presence of beryllium was also investigated. Design 407 is the same as design 406 (10 cm Be in natural Li), except that  ${}^6\text{Li}$  enrichment in lithium zones 5 (12 cm), 6 (10 cm), and 8 (7 cm) was increased to 50%. These results are also shown in table IV. The energy multiplication and tritium breeding ratio in design 407 are not significantly greater than in design 406. The reason is that design 407 is a poor configuration for efficient utilization of both beryllium and enriched lithium. An alternative design consisting of a 1 cm vanadium first wall, .5 cm 90% enriched lithium, 10 cm Be, 2 cm 90% enriched lithium, followed by a graphite reflector results in nuclear heating greater than 21 MeV per D-T neutron and a tritium breeding ratio of about 1.1. Such a system would have the important advantage of higher tritium production density; thus facilitating extraction and potentially reducing the tritium inventory. A detailed study of such systems minimizing lithium and beryllium volumes will be presented in another paper.

#### IV. Reflector Region

Lithium is less efficient in moderating high energy neutrons than some light and most heavy materials. Therefore, it is beneficial to keep the lithium



region to a minimum size for adequate tritium regeneration and follow it by a region of more effective moderator. This latter region can be called a reflector and serves as an intermediate region between the high power density blanket and the shield. The reflector is required to: 1- moderate and reflect a large fraction of the neutrons back into the lithium region increasing the tritium production per unit volume and allowing a thinner lithium region to be employed; 2- extracts nearly all the remaining kinetic energy from the neutrons thus decreasing the energy leakage into the shield; and 3- multiplies the energy production--if possible.

Graphite has been widely used for neutron moderating applications and has been proposed for use in fusion reactors. Iron, on the other hand, has considerably better neutron attenuation characteristics and the possibility of using it in the reflector region is explored here. In order not to perturb the magnetic field it is necessary that the materials employed be nonmagnetic. Hence, stainless steel which has more than 70% iron and is nonmagnetic should be used. Further, the nickel and chromium contents of stainless steel are useful for covering the well known iron "windows" associated with the minima in its total cross section.

To bring out the salient points in comparing graphite and SS in the reflector region, neutronics and photonics calculations were carried out for a system consisting of a 1 cm Nb wall, 40 cm of 95% Li plus 5% Nb structure, a 25 cm reflector region, and a one meter shield of 50% Pb + 20% Fe + 30%  $B_4C$ . The calculations were run for three designs using graphite, iron, and a mixture of 20% Fe + 50% Pb + 30%  $B_4C$ , respectively, in the reflector region. Iron was used in this series of calculations for the purpose of comparison but stainless steel does not change the results significantly.<sup>2</sup>

Table V compares the most important neutronics and photonics parameters for the three designs. Three important conclusions can be reached from these results: 1- Replacing graphite by iron in the reflector region increases the recoverable energy by about 9.5%; 2- The total (neutron plus gamma) energy leakage from the iron is about an order of magnitude lower than that from the graphite reflector; 3- A mixture consisting of 50% Pb plus 20% Fe plus 30%  $B_4C$  is better than graphite in the reflector region from the energy attenuation and multiplication of recoverable energy points of view but iron is better than either. The tritium breeding ratio drops to 1.06, which is unacceptable in one-dimensional calculations, when this mixture is used. In addition, the heat generation in the reflector region is so high that it would be difficult to employ lead in this region because of its low melting point.

From the above results, iron is superior to graphite in the reflector region from both an energy multiplication, and a neutron and gamma attenuation point of view. In addition, graphite suffers from severe radiation damage, mainly dimensional changes, when irradiated to fluences higher than  $10^{22}$  n/cm<sup>2</sup> while stainless steel has better radiation resistance at such fluences. Hence, stainless steel is superior to graphite in the reflector region. The only question remaining to be answered is the effect of cost considerations. Since no quality control is required in fabricating the stainless steel for this region, its cost is roughly the same as that of graphite. In addition, the gain in energy multiplication would offset the increase in cost even if stainless steel prices were higher. Furthermore, the stainless steel thickness required to perform the function of a 25 cm graphite region is roughly 9 cm. If the cost of the 9 cm stainless steel region were the same, there is still a benefit from using stainless steel since the shield and magnet volumes would be decreased by decreasing their inner radii.

A final point about the reflector concerns reactor safety. Lead which is likely to be employed in the shield region<sup>1</sup> has a low melting point. In case of a loss of coolant accident, high intensity neutron radiation will penetrate directly into the shield causing it to melt unless an efficient attenuator such as stainless steel is employed in the reflector region.

## References

1. M. A. Abdou and C. W. Maynard, "Nuclear Design of the Magnet Shield for Fusion Reactors," Proceedings of the First Topical Meeting on the Technology of Controlled Nuclear Fusion, CONF-74040, April '74 (these proceedings).
2. M. A. Abdou, "Calculational Methods for Nuclear Heating and Neutronics and Photonics Design for CTR Blankets and Shields," Ph.D. Thesis; University Microfilms Inc. 74-8981; also issued as Nuclear Engineering Department, Univ. of Wisconsin reports UWFD-66 and UWFD-67 (July 1973).
3. J. R. Powell, F. T. Miles, A. Aronson, and W. E. Winsche, "Studies of Fusion Reactor Blankets with Minimum Radioactive Inventory and with Tritium Breeding in Solid Lithium Compounds," Brookhaven National Laboratory, BNL-18236 (June 1973).
4. Don Steiner and A. P. Fraas, "Preliminary Observations on the Radiological Implications of Fusion Power," Nuclear Safety, 13, 5 (Sept. - Oct. 1972).
5. W. W. Engle, Jr., "A User's Manual for ANISN," K-1693, Oak Ridge Gaseous Diffusion Plant (March 1967).
6. M. K. Drake, Editor, "Data Formats and Procedures for the ENDF Neutron Cross Section Library," BNL-50279 (Oct. 1970). See also J. Ozer and D. Garber, "ENDF/B Summary Documentation," BNL 17541 and ENDF-201 (July 1973).
7. R. Q. Wright et.al., "SUPERTOG: A Program to Generate Fine Group Constants and  $P_n$  Scattering Matrices from ENDF/B," ORNL-TM-2679 (1969).
8. J. R. Knight and F. R. Mynatt, "MUG: A Program for Generating Multigroup Photon Cross Sections," CTC-17, (Jan. 1970).
9. M. A. Abdou, C. W. Maynard, and R. Q. Wright, "MACK: A Computer Program to Calculate Neutron Energy Release Parameters (Fluence-to-kerma factors) and Multigroup Neutron Reaction Cross Sections from Nuclear Data in ENDF Format," UWFD-37 and also ORNL-TM-3994 (July 1973).
10. S. Pearlstein, "Neutron-Induced Reactions in Medium Mass Nuclei," Journal of Nuclear Energy, 27, 81 (1973).
11. D. J. Dudziak et.al, "LAPHANO; A,  $P_0$  Multigroup Photon-Production Matrix and Source Code for ENDF," LA-4750-MS, also ENDF-156 (Jan. 1972); also W. E. Ford III, Oak Ridge National Laboratory, Private Communication (December 1972).
12. M. A. Abdou, "Calculational Methods for Nuclear Heating; Part II- Applications to Fusion Reactor Blankets and Shields," to be published in Nuclear Sc. Eng.
13. M. A. Abdou and R. W. Conn, "A Comparative Study of Several Fusion Reactor Blanket Designs," to be published in Nucl. Sc. Eng.
14. G. Kulcinski, D. Doran, and M. Abdou, "Comparison of Displacement and Gas Production Rates in Current Fusion and Future Fusion Reactors," to be published in the Proceedings of the Seventh ASTM International Symposium on Effects of Radiation on Structural Materials, Gatlinberg, Tenn. 11-13, 6-74.
15. B. R. Leonard, Jr., "A Review of Fusion-Fission (Hybrid) Concepts," Nucl. Tech. 20, 161 (Dec. 1973).
16. J. Cameron, Univ. of Wisconsin - Private Communication.

Table I  
Comparison of Tritium Breeding  
and Nuclear Heating for Various Structural Materials

		Niobium	Vanadium	St. Steel	SAP
${}^6\text{Li} (n, \alpha) t$	$T_6$	0.7734	0.9042	0.8161	0.7555
${}^7\text{Li} (n, n' \alpha) t$	$T_7$	0.4918	0.5547	0.4944	0.5970
Tritium Breeding Ratio†	T	1.2652	1.4589	1.3105	1.3525
	Zone				
Neutron Heating in MeV per D-T neutron	3	0.1275	0.2208	0.6016	0.5639
	4	6.1367	6.9487	6.4003	6.7733
	5	2.1180	2.4352	2.1895	2.3876
	6	1.4315	1.6445	1.4734	1.6060
	7	0.3330	0.2958	0.3204	0.4297
	8	0.1615	0.1805	0.1608	0.1769
	S*	10.3082	11.7255	11.1458	11.9374
Gamma Heating in MeV per D-T neutron	3	1.5361	0.4881	0.7732	0.2577
	4	1.7399	0.9494	1.2061	0.8830
	5	0.6781	0.4135	0.4809	0.4016
	6	0.4247	0.2766	0.3058	0.2775
	7	2.1933	2.0718	1.8749	2.5238
	8	0.0120	0.0093	0.0023	0.0075
	S*	6.5841	4.2087	4.6432	4.3511
Total Nuclear (neutron plus gamma) Heating in MeV per D-T neutron	3	1.6635	0.7089	1.3748	0.8216
	4	7.8765	7.8981	7.6064	7.6563
	5	2.7961	2.8487	2.6704	2.7892
	6	1.8562	1.9211	1.7792	1.8835
	7	2.5263	2.3676	2.1953	2.9535
	8	0.1735	0.1898	0.1631	0.1844
	S*	16.8921	15.9342	15.7890	16.2885

† $T_6$ ,  $T_7$ , and T for the blanket employing molybdenum are 0.843, 0.506, and 1.349, respectively.

\*sum over zones 3 through 8.

Table II

Comparison of Gas Production and Atomic Displacement  
Rates for Various Structural Materials

(all responses except displacements are given in units of reaction per fusion neutron)

	Zone	Niobium	Vanadium	St. Steel	SAP
$(n,\alpha) \times 10^4$	3	9.4470	28.9301	124.960	166.590
	4	4.3312	12.3060	55.1620	87.942
	5	0.9119	2.2741	10.3739	20.922
	6	0.4181	1.0062	4.6977	10.164
	S*	15.117	44.536	194.430	285.826
$(n, n'\alpha) \times 10^4$	3	N	N	N	20.459
	S*	N	N	N	35.158
$(n,P) \times 10^4$	3	31.985	54.179	258.198	117.886
	4	15.423	27.168	120.252	68.261
	5	3.440	6.203	26.478	18.007
	6	1.601	2.915	17.909	8.728
	S*	52.482	90.522	415.850	213.232
$(n, n')P \times 10^4$	3	N	N	69.958 <sup>a</sup>	207.482
	S*	N	N	127.523 <sup>a</sup>	328.752
$(n,d) \times 10^4$	3	N	N	N	31.096
	S*	N	N	N	49.472
$(n,t) \times 10^4$	3	N	N	N	0.140
	S*	N	N	N	0.208
displacements per atom per $10^{21}$ fusion neutrons	3	5.15	8.3	7.0	10.0

\* sum over zones 3 through 8.

N - indicates no data provided for this reaction in ENDF/B3 evaluations. For Molybdenum, N applies for all reactions in the table.

a - contribution of nickel and chromium only; N for iron.

Table III

Comparison of Gas Production (in appm/year/(MW/m<sup>2</sup>)) and Atomic Displacements (in dpa/year/(MW/m<sup>2</sup>)) Rates in the First Wall for Nb, V, SS, SAP, and Mo

	Niobium	Vanadium	St. Steel	SAP	Mo
Helium	23.7	56.1	203.3	408.6	48.5†
Hydrogen Isotopes	80.4	105.1	537.52	779.0	97.7†
Displacements*	7.2	11.6	9.8	14.0	8.3

\*displacement cross sections were derived using mean displacement energies of 60, 40, 40, 26 eV for Nb, V, SS, and Al respectively, and  $\beta = 0.8$  as explained in reference 14.

†calculated with cross sections from computer program THRESH<sup>10</sup>.

Table IV

Effect of Enriching Lithium in  $\text{Li}^6$  and Adding Beryllium on  
Tritium Breeding and Energy Multiplication in the Blanket Shown in Figure 1  
(Results are normalized to one fusion neutron)

Design ID	401	402	403	404	405	406	407
a/o of $\text{Li}^6$ in lithium	7.42*	15.0	30.0	50.0	7.42*	7.42*	50.0†
v/o of Be in blanket	0.0	0.0	0.0	0.0	9	20	20
Neutron Heating in							
$\text{Li}^6$	4.9966	6.1338	7.6839	9.3943	6.4462	7.9520	8.6001
$\text{Li}^7$	6.0376	5.4082	4.3270	2.9924	4.7795	3.5067	3.1918
V	0.3953	0.3750	0.3590	0.3481	0.3756	0.3528	0.3452
Fe	0.2340	0.2278	0.2208	0.2153	0.1507	0.0774	0.0720
Ni	0.0801	0.0785	0.0765	0.0749	0.0519	0.0269	0.0250
Cr	0.0538	0.0521	0.0502	0.0487	0.0347	0.0179	0.0164
Be	0.0	0.0	0.0	0.0	2.2193	4.3891	4.4100
Total Neutron Heating (MeV)	11.7974	12.2754	12.7174	13.0737	14.0579	16.3497	16.6605
Total Gamma Heating (MeV)	4.2533	3.7893	3.3851	3.0627	3.4891	2.6623	2.3778
Total Heating (MeV)	16.0507	16.0647	16.1025	16.1364	17.5470	19.0120	19.0383
Tritium Breeding	0.9042	0.9901	1.0529	1.0878	1.2361	1.5803	1.6369
T <sub>6</sub>	0.5547	0.5013	0.4052	0.2824	0.4410	0.3249	0.2989
T <sub>7</sub>	1.4589	1.4914	1.4581	1.3702	1.6771	1.9052	1.9358

\*Corresponds to natural lithium

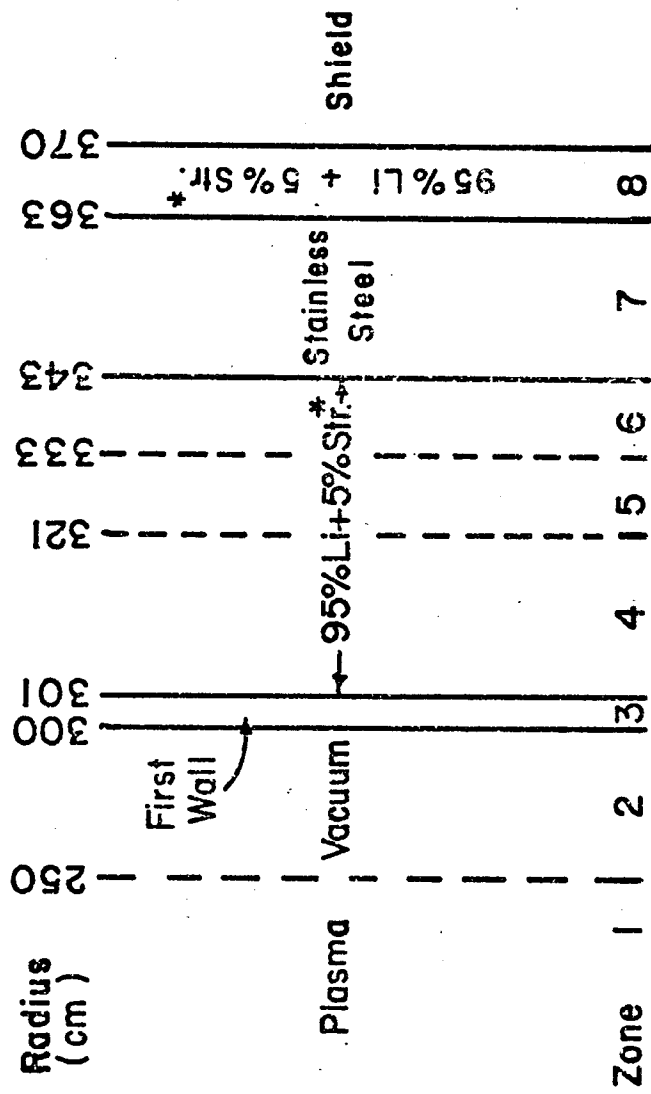
†50.0 a/o  $\text{Li}^6$  in lithium zones 5 (12 cm), 6 (10 cm), and 8(7 cm); zone 4 (20 cm) is natural lithium

Table V

Comparison of Various Materials in the Reflector Region

Reflector Material	Graphite	20% Fe + 50% Pb + 30% B <sub>4</sub> C	Iron
Neutron Heating*	10.6659	10.6585	10.1790
Gamma Energy Production*	5.1714	5.6580	6.8217
Gamma Heating*	4.8306	5.6481	6.794
Total Heating	15.4965	16.3073	16.9731
Neutron Energy Leakage* from reflector	0.2794	0.0914	0.0616
Gamma Energy Leakage* from reflector	0.3399	0.0025	0.0257
Total Energy Leakage*	0.6193	0.0939	0.0873
Li <sup>6</sup> (n,α)t	0.7707	0.5808	0.7645
Li <sup>7</sup> (n,n'α)t	0.4877	0.4850	0.4836
Tritium Breeding Ratio	1.2584	1.0658	1.2481

\* in MeV per D-T neutron



\* Materials for first wall and structure are as follows:

Design 301: Niobium, Design 302: Vanadium,

Design 303: Stainless Steel, Design 304: SAP

Figure 1. Reference Design for Comparison of the nuclear performance of Several materials for first wall and structure.



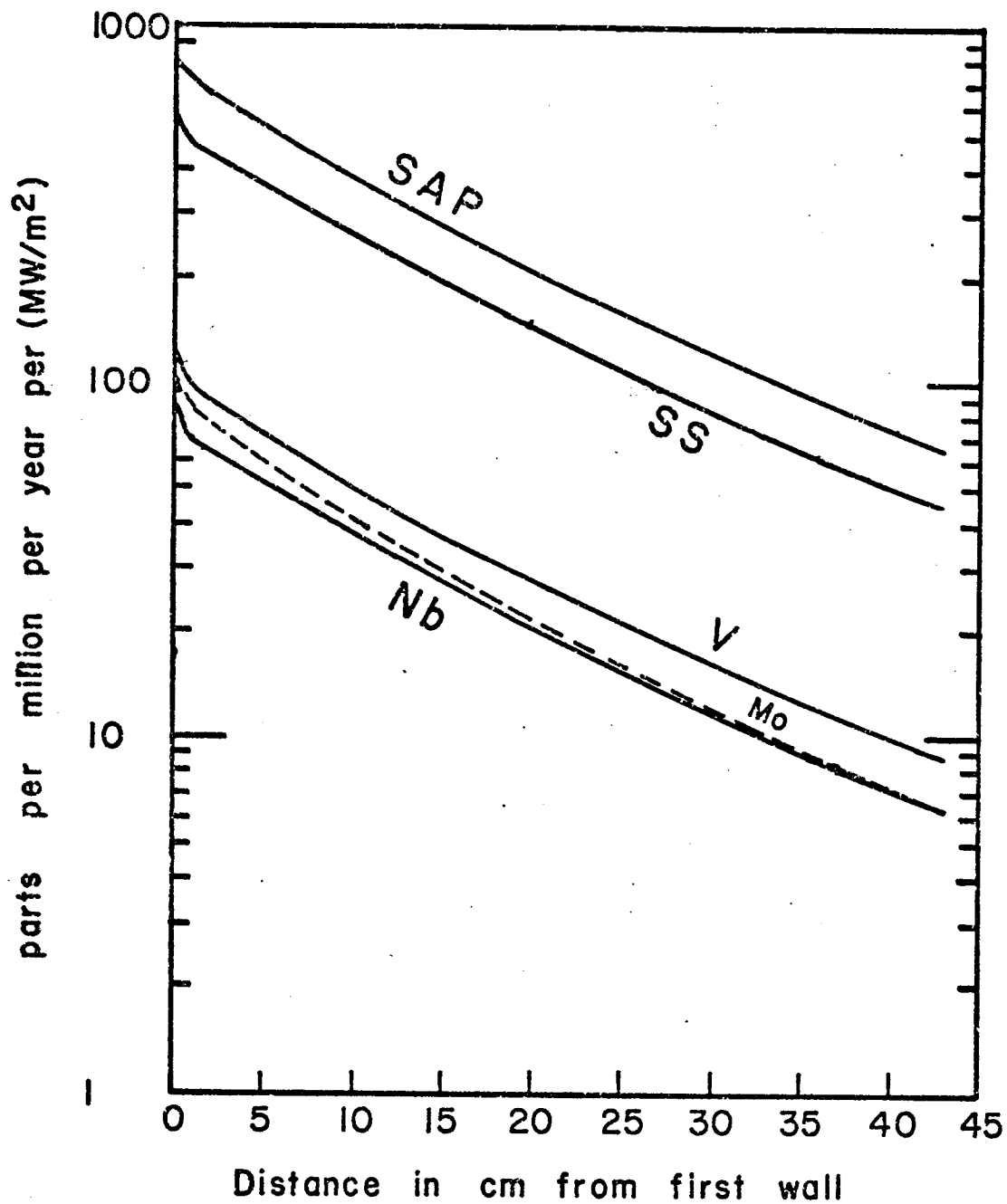


Fig.2 Spatial distribution of Hydrogen isotopes production in Niobium, Vanadium, Stainless Steel, SAP, and Molybdenum.

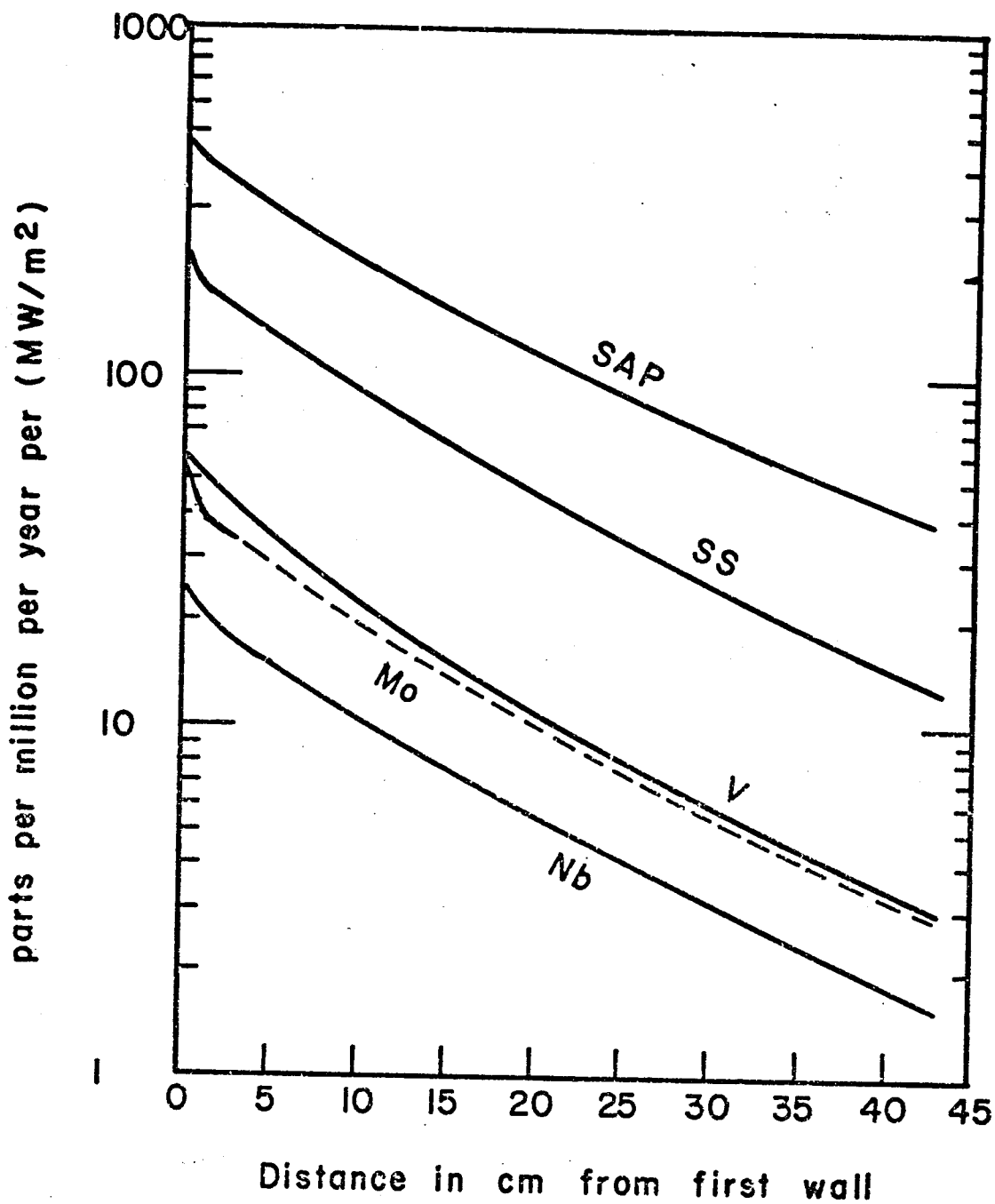


Fig. 3 Spatial distribution of Helium production rate in Niobium, Vanadium, Stainless Steel, SAP, and Molybdenum.

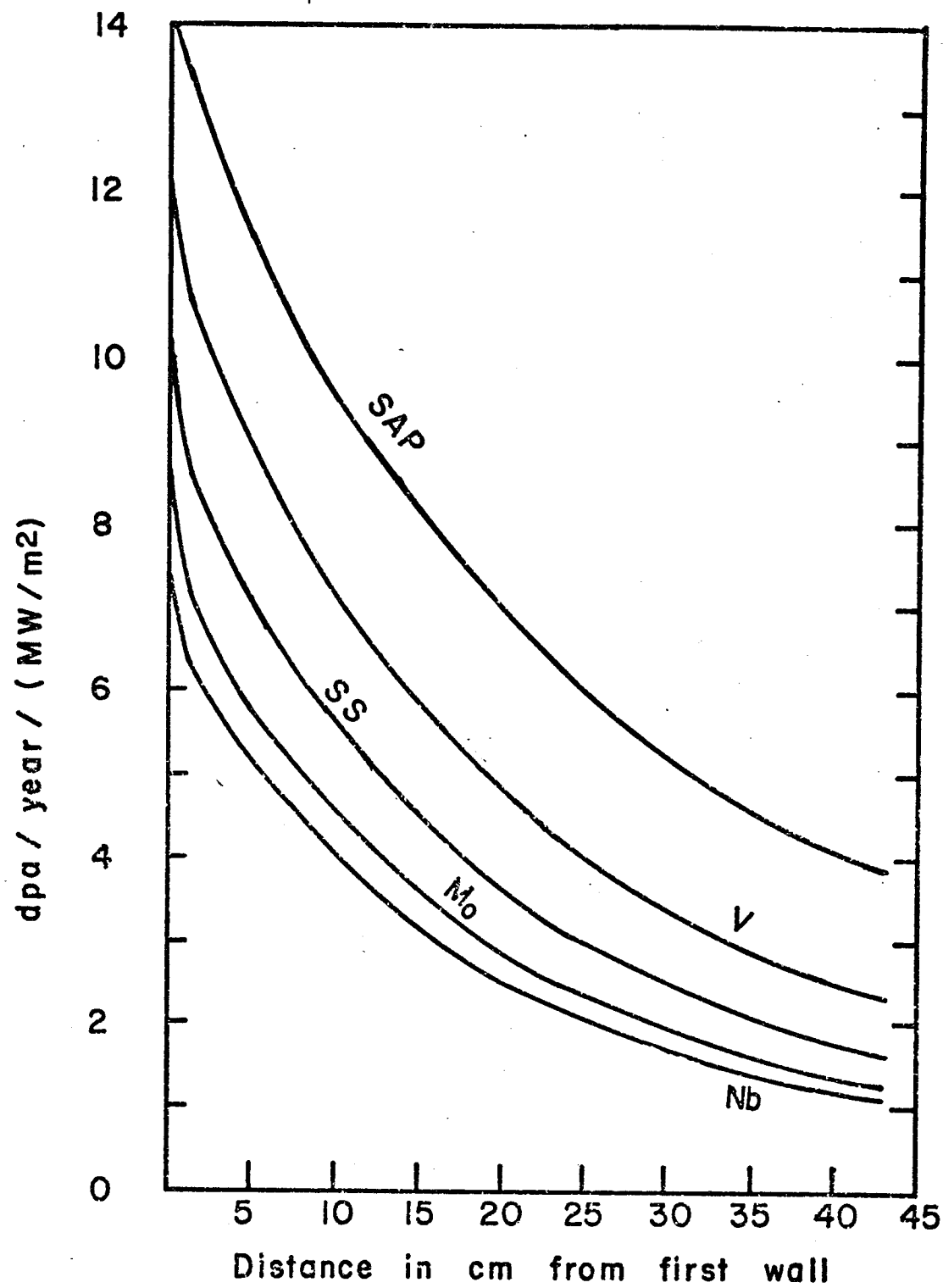


Fig.4 Spatial distribution of atomic displacements in Vanadium, Niobium, Molybdenum, Stainless Steel, and SAP.